CLM-P 400

ABLATION OF SOLID HYDROGEN BY ELECTRONS AND IONS

by

R. CLAMPITT

(Submitted for publication in Nuclear Fusion)

SUMMARY

Results of experiments are presented on the interaction of low energy electrons and ions with hydrogen condensed on a metal surface. Observations are made on the following: desorption of gas and ejection of hydrogen-cluster ions by electrons; ablation of the surface by scattered alkali ions; field evaporation of positive ions from the solid; electron-ion recombination. The results are relevant to current work on ablation of hydrogen pellets by plasma.

UKAEA Research Group
Culham Laboratory
Abingdon
Oxon

June 1974

CONTENTS

1. INTRODUCTION

Accelerated deuterium-tritium pellets are proposed for refuelling a fusion plasma. Experiments are currently in progress on hydrogen pellet ablation by a plasma[1].

The results of some experiments on the interaction of low energy electrons and ions with solid hydrogen are presented below. The experiments were not directed, at the time of execution†, towards the pellet charging and ablation problem, and thus are incomplete. Nevertheless the results should be helpful in the current work.

2. EXPERIMENTAL METHODS

A schematic diagram of the apparatus is shown in figure 1. Hydrogen gas is condensed on a copper surface in a vacuum of $\sim 10^{-10}$ torr. The temperature of the surface can be controlled accurately between 2^{o} K and 4.2^{o} K by means of a liquid-helium cooled cryostat.

For electron studies a focussed electron beam of 2×10^{-8}A is swept over the surface by sawtooth voltages on X and Y plates, so as to distribute the charge accumulated during the experiment.

For ion studies a beam of H_2^+ ions (< keV) of $\sim 10^{-10}$A can be directed at the target from a mass spectrometer, or alkali metal ions from coated filaments nearby. Accumulated positive charge at the surface is neutralised with electrons from another filament.

Secondary ions emerging from the surface are focussed either into a mass spectrometer for spectral analysis or else into a cup. Ultra-violet photons can be detected by a photomultiplier fitted with a LiF window and tungsten cathode. An optical absorption cell is provided to filter the emitted radiation.

The velocity distribution of hydrogen gas desorbed by electrons could be obtained by pulsing the incident electron beam, detecting the molecules by ionisation in the mass spectrometer and processing these as a time-of-flight spectrum with a time-to-height convertor and pulse-height analyser.

3. RESULTS AND DISCUSSION

3.1 Electron impact of solid hydrogen

3.1.1 Ejection of positive ions

Electron excitation of solid hydrogen can result in ejection of positive ions into the gas phase.[2] In the experiments reported here the solid hydrogen is formed on a cold metal support. Consequently in order to avoid confusion in interpreting ion spectra we must first know about electron ionisation of the atoms on the 'hydrogen-free' metal surface.

A typical mass spectrum of positive ions ejected from the copper substrate in ultra-high vacuum is shown in figure 2. It is seen that the surface is covered mostly with chemisorbed hydrogen atoms, and fluorine atoms derived from the bulk of the copper.[3]
When molecular hydrogen is condensed onto this surface at 3^{o}K, hydrogenic ions are ejected from the surface and we have shown [2] that the most likely processes leading to ejected ions are

$$e + H_2 \rightarrow H^+ + H$$

$$H^+ + H_2 + H_2 \rightarrow H_3^+ + H_2$$

$$H_3^+ + (H_2)_n \rightarrow H_3^+ (H_2)_{n-1} + H_2$$

where the proton gains kinetic energy from dissociative ionisation of H_2 (figure 3).

Whereas the major ion-forming process in the gas phase is

$$e + H_2 \rightarrow H_2^+ + 2e$$

molecular ions so formed in the solid do not gain sufficient kinetic energy to escape from the surface, in the absence of electric field gradients (c.f section 3.4), and remain trapped.

The ion spectrum exhibits a prominent ion at H_{15}^+ which might well be $H_3^+ (H_2)_6$. Figure 4 shows the intensity distribution of ejected cluster ions for n > 10. It may not be coincidence that the break in the curve

†1968-69

occurs at a value of n close to that for a hexagonal close-packed crystal (n=13), which form hydrogen usually assumes when condensed from the gas phase.[33] Thus we might be observing here the ejection of a crystallite of hydrogen attached to an ion.

A high current electron beam changes considerably this characteristic ion spectrum; this might correspond to disruption of the ordered lattice.

If a positive electric field is applied between the solid and ground potential ($\geq 10V.cm^{-1}$) during electron bombardment, H_2^+ ions can escape by field evaporation both clustered and unclustered. The ion H_6^+ is a particularly prominent even-mass cluster ion.[4]

An ejected ion spectrum for deuterium is shown in figure 5a. Here also D_{15}^+ is a particularly significant ion. The intensity distribution differs from that of solid hydrogen maybe because of differing polarisabilities of the nucleated molecules and ionic radii of the postulated nucleating centres, H_3^+ and D_3^+.

We could not obtain a characteristic ion spectrum as for hydrogen. Figure 5b shows a deuterium ion spectrum obtained in a separate experiment. Here the D_7^+ is prominent and the D_{15}^+ ion clearly more abundant than D_{14}^+ and D_{16}^+.

Of the unlabelled ions in the deuterium spectra three of them are probably $D^+(H_2O)$, $D^+(HDO)$ and $D_3^+(H_2O)$ at respectively m/e20, 22 and 24. The ion at m/e 16 could be O^+ from the water impurity though it is uncommonly abundant. It is not clear why there should have been much more water contamination here than in the hydrogen experiments. One might suppose that these are not water clusters at all but the ions $D_2^+(D_2)_n$ with n = 3-5. An unambiguous explanation of the composition of these ions is of interest insofar as if they are deuterium ions, based on a D_2^+ nucleus, then we will have demonstrated their much greater stability vis à vis the H_2^+ based ions.

The multiplicity of hydrogenic ions from a D_2/H_2 mixture is reminiscent of, though must not be mistaken for, hydrocarbon 'cracking patterns' in conventional mass spectra.

We have observed a curious effect of impurity gases on the electron ablation rate of solid hydrogen. The efficiency of ion ejection by low energy electrons increases 10-20 times when neon or argon is condensed onto the solid during ablation. Unfortunately trace impurities such as H_2O and CO were observed to be condensed along with rare gas¶. These are ejected from the surface as H_3O^+ and HCO^+ respectively. Consequently we cannot at present offer an unambiguous explanation of this phenomena.

There is no precedent for ion spectra of this sort and the presence of impurities complicates enormously the identification of the ejected ionic species.

Indeed the complete and consistent absence of an ion at some particular value of m/e, such as m/e 34 in the spectra from solid H_2 contaminated with N_2, should constitute a fundamental clue as to the composition of adjacent ionic species. Even with this information, however, we still cannot unequivocally assign identities to most impurity ions.

Some ions are fairly common in our experiments and readily identifiable, e.g. HCO^+ and H_3CO^+ from CO-doped H_2;* or the water cluster ions of the type $H_3O^+(H_2O)_n$ with n = 1-6

¶ These are generated in the ion pump of the apparatus when rare gases in particular are introduced.

* The formaldehyde ion has recently been detected in the interstellar medium in the vicinity of cold hydrogen clouds and interstellar grains.[8] Certainly there is a mechanism for its production, i.e. photo-ionisation of solid hydrogen grains containing CO impurity.

3.1.2 Ejection of Negative Ions

Some brief experiments on negative ions are reported here.

First we look at the 'bare' target surface, in the absence of solid H_2.

The ions H^-, O^-, F^- and Cl^- are particularly abundant.

With frozen water impurity on the surface the variation of σ (H^-) with electron energy shows remarkable similarity to that observed in the gas phase: [9]

$$e + H_2O \rightarrow H^- + OH$$

and is shown in figure 6.

Similarly with solid hydrogen, the variation of $\sigma(H^-)$ with electron energy is similar to that observed in the gas phase[10] (figure 6).

An ion at m/e 2 of about one tenth the intensity of H^- was observed. This could not readily be attributed to D^- impurity. The intensity was dependent on gas phase pressure of H_2, in contrast to all the usual ions of surface origin. If the ion is H_2^-, whose existence has evoked much speculation,[11] then it would appear to be formed by a charge-exchange process near the surface. The cross-section for the process $H^- + H_2 \rightarrow H_2^- + H$ is not reported. That for the resonant charge-exchange process:

$$H^- + H \rightarrow H^- + H$$

is very high, $3 \times 10^{-14} cm^2$, at 1eV.[12]

Alternatively it might be that the H_2 molecule, incident on the electron-rich surface, captures an electron there to form a stable state of H_2^- of extremely low binding energy.

It would be of considerable interest to repeat these experiments in order to verify or refute the observation of a stable state of H_2^-.

We have not detected ion clusters of the type $H^-(H_2)_n$ though this may be due to insufficient sensitivity of the detection system: the cross-section for H^- production from H_2 is many orders lower than that for H^+.

3.1.3 Desorption of Gas Molecules by Electrons

The number of H_2 molecules desorbed from a thick (>50 monolayers) layer of solid hydrogen at 3^oK by electrons of 20eV was obtained by measuring pressure rise on an ion gauge and taking account of the gauge sensitivity and the pumping speed of the cold target ($44.2\ \ell.sec^{-1}cm.^{-2}$). The value is 45 molecules/electron at 20eV, subject to an error of about 25%. This can be compared with reported values[34] of 1000 mol/elect. for 2keV electrons and 50,000 mol/elect. for 5keV protons.

The velocity distribution of the desorbed gas molecules was obtained by the method described in Section 2. The apparatus was not specifically designed for this experiment, viz: the detector was not differentially-pumped or shielded from the target, and the flight length from target to detector was only 2.8cm. Consequently spectra were masked by background. The time-resolved component of the ion signal was recovered by operating the pulse-height analyser alternately in 'add' and 'subtract' modes. Allowance was made for the ion transit time through the mass spectrometer (2.5μs.) which was measured in a separate experiment.

Time-of-flight spectra are shown in figure 7 for three values of electron energy. Theoretical curves of the velocity distribution would take account of all modes of interaction between the electron and H_2 lattice[29] and would be a complicated exercise. None of the curves fit a simple v^2 distribution nor a v distribution based on an exponential dissipation of energy. However the experimental arrangement was somewhat crude and we do not know to what extent background gas distorts the observed curves. A more refined experiment is needed to establish unequivocally the exact form of the velocity distribution.

If we assume a v^2 distribution for the desorbed gas then the most probable velocity for 40eV incident electrons is 2.4×10^4 cm.sec^{-1}; and for 90eV electrons 4.8×10^4 cm.sec^{-1}.

3.2 Ion Scattering from Solid Hydrogen

This part of the study was restricted mostly to alkali ion scattering.

For 8eV Li^+ ions (typically 2×10^{-10}A) incident at 45° on a thick layer of hydrogen the reflection coefficient was 0.2. However some of these scattered ions emerge not as Li^+ but as ion-induced dipole clusters of the type $Li^+(H_2)_n$ with n lying mostly between unity and six (Figure 8). These observations have already been reported. [13]

Other alkali ions emerge similarly clustered from the surface.[5] Figure 9 shows comparisons of alkali-hydrogen spectra. As the ionic size Z increases more molecules can be accommodated.¶

Thus the efficiency with which ions can ablate solid H_2 by cluster-ion scattering, increases with ionic radius. We have some evidence, which requires substantiating, that with increasing Z of the alkali ion the clustered-to-unclustered ratio of scattered ions increases until for Cs^+ (10eV) it is 0.5.

Ion spectra resulting from Li^+ impingement onto contaminated solid H_2 exhibit many ions up to m/e 200 and interpretation of composition is too difficult at present.

Low energy (25-200eV) H_2^+ ions incident on solid H_2 are trapped until the potential of the surface attains that of the incident ions which are then repelled and no longer reach the surface. We have not measured the reflection coefficient of hydrogenic ions from solid hydrogen.

We could not detect ion clusters from incident H_2^+ though this might be due to inadequate sensitivity of the detector.

¶ The stereospecificity of molecules clustered on ions e.g. $H_3^+(H_2)_6$ and $Li^+(H_2)_6$ was reinforced by observations [13] of neon atom-clustering on Li^+ where the shell appears complete at $Li^+(Ne)_6$.

3.3 Electron-Ion Recombination in the Solid

It was shown that ultra-violet photons are produced when the temperature of solid H_2, previously implanted with H_2^+ and electrons, is increased from $3^\circ K$ to $4.2^\circ K$. The light emission coincides with charge movement through the solid into the vacuum and in the opposite direction to the metal support.

By interposing a cell of pure dry oxygen at two atmospheres pressure (a Lyman-α window) between the target and the photon detector it was found that some of the emitted radiation was Lyman - α (1216Å) arising most likely from dissociative recombination.

$$H_2^+ + e \rightarrow H_2^* \rightarrow H(2S,2P) + H(1S)$$

When 20eV H_2^+ ions only were implanted into solid hydrogen at $3^\circ K$ and the solid then warmed to $4.2^\circ K$ photons were detected at the same time as ion flow to the metal substrate. These probably arise from neutralisation and de-excitation of the H_2^+ ions at the substrate. The photon flux from this experiment was several orders of magnitude lower than resulted in the former case.

The onset of charge mobility in solid H_2 is so rapid, occurring in the region of $4^\circ K$, that it was not possible to detect any difference in ion and electron mobilities. However when H_2^+ and electrons were implanted into solid neon, the onset of electron and ion mobility could be separately identified [31]. Also in a neon matrix it was observed that ion-electron recombination (evidenced by photon emission) precedes ion evaporation.

The interpretation as recombination was reinforced by separately implanting (a) only 6eV electrons and (b) only 25eV H_2^+ ions, when for (a) there was observed negative charge evaporation and no photons, and for (b) positive charge evaporation and no photons.

3.4 Field Evaporation of Ions from Solid Hydrogen

Low energy H_2^+ ions of 70eV were trapped in solid hydrogen at 3^oK by directing the ions onto the metal substrate during condensation of H_2 from the gas phase. Electrons of nominally ∿leV were simultaneously directed at the target. Subsequent application of a positive potential of 100V ($E \sim 100V.cm^{-1}$) in the absence of the primary beams, results in the evaporation of positive ions from the surface into the vacuum. The emission can be sustained for several minutes depending on the original ion dose.

A mass spectrum of the evaporated ionic species is shown in figure 10. These are cluster ions of the type observed by electron impact on solid hydrogen (section 3.1). The mass distribution varies considerably during the emission period.

It is interesting that H_2^+ is prominent i.e. that it can survive in solid hydrogen without undergoing the reaction

$$H_2^+ + H_2 \rightarrow H_3^+ + H.$$

The cross-section σ for this process, varies at low ion velocities as $\sigma \propto 1/v$ and is reported by experiment[14] to be 36Å^2 at 0.1eV.

The resonant charge-exchange process

$$H_2^+ + H_2 \rightarrow H_2 + H_2^+$$

has not been measured at very low energies but an extrapolated theoretical value[15] at 0.1eV is about 10Å^2. Our observations of H_2^+ indicate that a considerable fraction of H_2^+ ions move through solid hydrogen by resonant charge-exchange and can emerge through the surface-vacuum interface without undergoing the bimolecular dissociative process.

Deposition of up to 200 layers of H_2 onto the surface during ion evaporation did not significantly alter the ion intensities. The ionic mass distribution was too erratic to detect any change on deposition of H_2. At about 400 monolayers of overlaid H_2 ion evaporation ceased abruptly.

There was some indication that the mean size of the ion cluster increased as evaporation proceeded.

The temperature-dependence of the evaporation rate of several cluster ions was obtained by rapidly changing the substrate temperature, thereby minimising errors in intensity measurement due to the erratic nature of the evaporation process.[31] The results are shown in figure 11.

The theory of charge evaporation from insulating solids (Appendix) predicts that for charges in the bulk of the solid the eveporation rate k will vary as

$$k \propto \exp(-E_A/kT)$$

where E_A is the activation energy for evaporation.

The experimental data are in accordance with the predicted temperature-dependence and give $E_A/k = 5.4^oK$.

The only previous work for comparison is the field evaporation of negative charge (mass unknown) from liquid helium[16] for which $E/k = 25^oK$.

It has long been postulated that ions in liquid helium exist as cluster ions of perhaps 40-50 atoms,[17] but there is no previous experimental evidence that this is so. We have shown by mass-identification of the evaporated ions that most are indeed clustered in solid hydrogen.

4. CONCLUSIONS

This work has demonstrated one mechanism of ablation of solid hydrogen by low energy electrons and ions, i.e. cluster-ion ejection. There is insufficient data to assess the significance of this ablation process in relation to others, such as thermal desorption.[34] But it will merit consideration in any shielding phenomena at the pellet-plasma boundary.

Positive ions are evaporated from the bulk solid in weak electric fields. The rate of ion evaporation is slow in

relation to the time required to accelerate a charged pellet into a plasma.

If the behaviour of electrons in solid H_2 is similar to electrons in helium then it is likely that a pellet charged negative by surface contact would lose its charge rapidly in an external electric field; electrons created or implanted in the bulk of the solid, however, would evaporate only slowly. Evaporation of positive surface charge might also be a slow process because of the possibility of cluster-ion formation.

It would be instructive to study the field evaporation of surface positive charge, and both surface and bulk negative charge, from the solid.

It should also be fruitful to measure charge mobility in the solid as a function of electric field strength and temperature, in order to obtain the maximum charge that can be accumulated and sustained in the presence of practical acceleration fields.

APPENDIX

THEORY OF ELECTRICAL CHARGES IN INSULATING SOLIDS

1. Introduction

We reported in section 3.4 that positive ions can be evaporated from solid hydrogen by an electric field. Evaporation of negative charge from liquid helium in electric fields has been observed and studied in the area of low temperature physics.[6,16,17]

Theoretical and experimental work on ions and electrons in liquid helium have been in progress for about fifteen years. The theory is equally applicable to insulating solids comprised of light atoms in which short-range Hartree-Fock electron-atom repulsion dominates over the long-range polarisation force.[18] It should be useful to give here elements of theory as applied to helium in order to understand our experimental observations.

1.1 Electrons in Insulating Solids

An electron approaching the surface of an insulating solid experiences an attractive image force resulting from an induced dipole in the surface. The polarisation potential $V(x)$ of the atom is related to the dielectric constant of the material ε by

$$V(x) = -\tfrac{1}{4}.e^2.(\varepsilon - 1)/(\varepsilon + 1) \quad ;$$

for values of x greater than the internuclear separation.

For surfaces having a negative electron affinity (e.g. He, H_2) there is a potential barrier which prevents the electron from entering the surface; for He it is typically $\sim$1eV. Thus there exist localised surface states for electrons just outside the surface. These are called 'image-potential-induced surface bands.'[19]

Theoretical values of the energy of the surface state electrons above the vacuum level for solid H_2 and D_2 are 3.27eV and 4.33eV respectively.[19]

This is the minimum kinetic energy that incoming electrons must possess in order to enter the surface.

In the case of electrons in He(II), electron-atom repulsion creates a bubble of $\sim$20Å radius,[20] in which the electron is localised. The total energy of formation of a bubble relative to an electron at rest in vacuo is 0.1 - 0.3eV. If an electric field is applied of such polarity to move the bubble to the surface it experiences an image force of approximately the same magnitude but of opposite sign to that on an electron outside the surface. At the surface the bubble formation energy will be dissipated to neighbouring atoms during bubble annihilation. The electrons now experience a potential minimum just inside the surface.

In a sufficiently high electric field the trapped electrons can move into the surface bands from which thermionic electron emission can occur. Electrons in the states just outside the surface are stable in fields so directed to move them into the surface. Fields of opposite sign remove the surface electrons in 10^{-4} - 10^{-6} seconds depending on the values of field and temperature.[28] The rate of evaporation of electrons is given by

$$q(t)/q_o = e^{-t/\tau}$$

where $q(t)$ is the charge remaining at time t and τ is related to its reciprocal, the evaporation rate constant k, by [21]

$$k \propto E^{-2} \exp(-A/E)$$

where E is the field strength.

An electron inside the surface will evaporate in some seconds, depending weakly on field and exponentially on temperature, e.g. for the helium: [21] $k(\text{sec}^{-1}) = 1$ at $1/T = 0.6\,^{\circ}K^{-1}$; and $k = 10^{-3}$ @ $1/T = 0.85\,^{\circ}K^{-1}$.

It has been found experimentally [22] that the mobility of electrons moving through the bulk of liquid helium is independent of T, but decreases two hundred-fold[7] when

the electric field increases from 0.4kV.cm^{-1} to 0.7 kV.cm^{-1}.

Electron (or ion) scattering within insulating solids is described in terms of Rayleigh waves.[23,26] It can be shown that the fractional momentum transfer rate for solid helium is $\sim 10^4$ times that for liquid helium.[23] This interesting fact means that electrons or ions in the solid are much more mobile and liable to escape than in the liquid.

1.2 Ions in Insulating Solids

All the foregoing arguments on electrons apply to ions except that ions are believed to exist in an electrorestrictive shell or ion cluster.[17] In the immediate vicinity of the ion the density of molecules in the solid will be higher than elsewhere because of the polarisation force. Any comprehensive theory of ion mobility in condensed media must account for this condensation shell.[24] So far however workers have used only the sphere-model of scattering to deduce scattering cross-sections for positive ions.[25]

The momentum loss per centimetre is

$$\lambda = (E) = eE/v \qquad \text{gm.sec}^{-1}$$

where E is the field gradient, v is the ion velocity.

Account must be taken of both phonon and roton scattering since the momentum imparted by ions to long wavelength phonons is relatively insignificant the latter being an order of magnitude higher.[26] The positive ion is considered to scatter sound like a classical hard sphere. For ^{4}He, λ is given by

$$\lambda = 1.5 \times 10^{30}.a^6.T^8$$

where a is the effective ionic radius; T is temperature. Using this approach an expression for the total momentum transfer cross-section can be obtained which gives a reasonable fit to the experimental data on ionic velocity in liquid helium.[25] It is found that helium ions in helium have an effective cross-section of 238$\mathring{A}^2$, corresponding to a large cluster ion.

Also,[27] for He^+ in He at low fields, $v \propto E$ i.e. the ion mobility μ is constant since $\mu \equiv v/E$; whilst at higher fields (>200V.cm^{-1}) v = constant $\simeq$60m.sec^{-1}.

The temperature-dependence of ionic mobility is given by [27]

$$\mu \propto \exp(\Delta/kT)$$

This relationship arises from the temperature-dependence of the roton number density n on temperature:

$$n \simeq \exp(-\Delta/kT)$$

where Δ is the energy required to thermally excite a roton and for ^{4}He it has approximately the same value for positive and negative ions. As an example, for He at 0.3°K μ is $\sim 10^5$ times greater than that at T_λ, the lambda point.

The rate of evaporation of ions from solid hydrogen would be expected to vary exponentially with temperature and to be essentially independent of applied field above $\sim$200V.cm^{-1}. The experimental data of figure 11 supports the predicted temperature-dependence though we have not obtained the electric-field dependence.

Finally the electron-ion recombination rate α in He(II) is found experimentally[6] to fit a model based on Langevin recombination. For ions and electrons in He, α is found to be inversely proportioned to temperature and has a value of 2 x 10^{-7}cm^3/ion.sec. at 1.94°K.

ACKNOWLEDGMENT

The author thanks L Gowland and D.K. Jefferies (Culham) for experimental assistance and Dr M A J Rodgers (Manchester) for unpublished data.

REFERENCES

1. Øster F., and Sillesen, A.H. 5th Europ. Conf. Controlled Nuclear Fusion Grenoble 1972, Vol. 1.

2. Clampitt, R. and Gowland, L. Nature 223, 815, 1969.

3. Clampitt, R. Proc. 2nd Adsorp. Desorp. Phenom. Florence, 1971, Acad. Press.

4. See also van Deursen, A., and Reuss, J. Int. J. Mass Spec. Ion Phys. 11,483,1973.

5. Clampitt, R. Xth Phenom. Ion Gases, Oxford, 1971; Invited Papers; Parsons Ltd. Oxford.

6. Careri, G., and Gaeta, F.S. VIIth Int. Conf. Low Temp. Phys. (Toronto) 1960, p.505.

7. Careri, G.et. al. IXth Int. Conf. Low Temp. Phys. Columbus. 1964.

8. Interstellar Dust and Related Topics. Ed. Greenberg and van de Hulst. Reidel 1973.

9. Schulz, G.J. J. Chem. Phys. 33, 1661, 1960.

10. Schulz, G.J. Phys. Rev. 113, 816, 1959.

11. See for example Taylor, H.S.E., Proc. Phys. Soc. 90, 877, 1967, et seq.

12. Hummer, D.G. et. al. Phys. Rev. 119, 668. 1960.

13. Clampitt, R. and Jefferies, D.K. Nature 226, 141, 1970.

14. Neynaber, R.H., and Trujillo, S.M. Phys. Rev. 167, 63, 1968.

15. Massey, H.S.W., and Gilbody, H.B. Electronic and Ionic Impact Phenom. Clarendon Press 1974.

16. Bruschi, L. et. al. Xth Int. Conf. Low Temp. Phys, (Moscow) 1969; 1, 219.

17. Atkins, K.R. VIIth Int. Conf. Low Temp. Phys. (Toronto), 1960, p. 519.

18. Miyakawa, T and Dexter, D.L. Phys. Rev. 184, 166, 1969.

19. Cole, M.W. and Cohen, M.H. Phys. Rev. Lett. 23, 1238, 1969.

20. Zipfel, C. and Sanders, T.M. XIth Int. Conf. Low Temp. Phys. Scotland, 1968.

21. Crandle, R.S. and Williams, R. Phys. Rev. (A) 5, 2183, 1972.

22. Schoepe, W. and Probst, C. Phys. Lett. 31A, 490, 1970.

23. Cole, M.W. Phys. Rev. (B), 2, 4239, 1970.

24. Shikin, V.B. Sov. Phys. J.E.T.P. 31, 936, 1970.

25. Schwartz, K.W. and Stark, R.W. Phys. Rev. Lett. 22, 1278, 1969.

26. Baym, G. et. al. Phys. Rev. Lett. 22, 20, 1969.

27. Meyer, L. VIIth Int. Conf. Low Temp. Phys. (Toronto), 1960, p. 487.

28. Crandle, R.S. Phys. Rev. (A) 9, 1297, 1974.

29. Bottiglioni, F., Coutant, J. and Fois, M. Phys. Rev. (A) 6, 1830, 1972.

30. Keto, J.W. Stockton, M. and Fitzsimmons, W.A. Phys. Rev. Lett. 28, 792, 1972; Phys. Rev. (to be published).

31. Rodgers, M.A.J.R. (unpublished work).

32. Careri, G. et. al. IXth Int. Conf. Low Temp. Phys. Columbus, 1964.

33. Barrett, C.S. et. al. J. Chem. Phys. 45, 834, 1966.

34. Erents, S.K. and McCracken, G.M. J. App. Phys. 44, 3139, 1973.

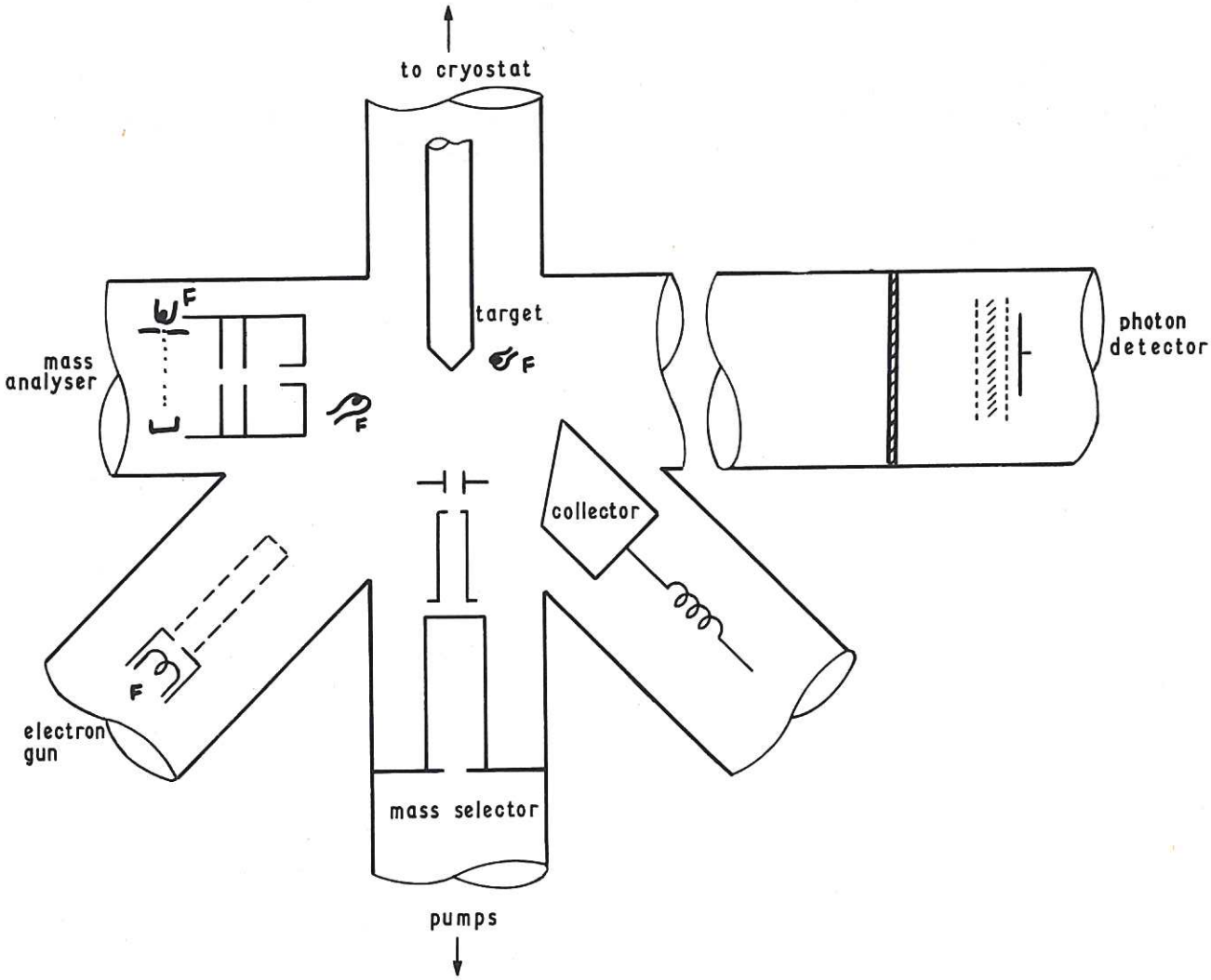

Fig.1 Schematic diagram of apparatus

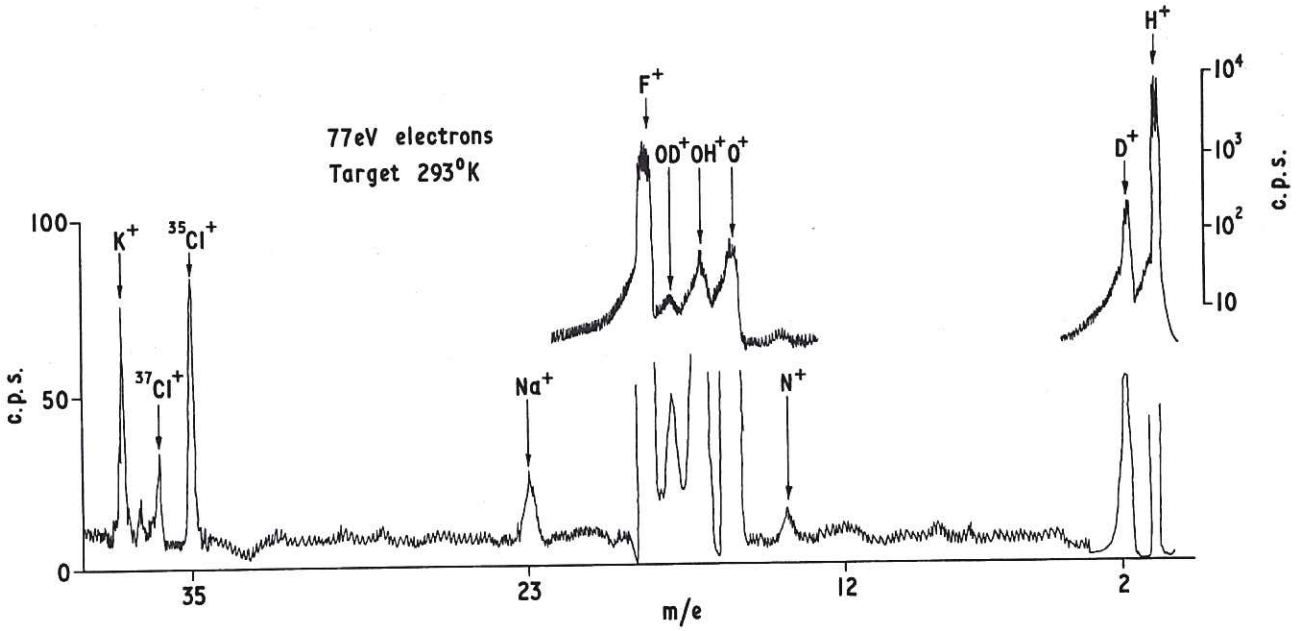

Fig.2 Ejected ion spectrum from copper surface

CLM-P400

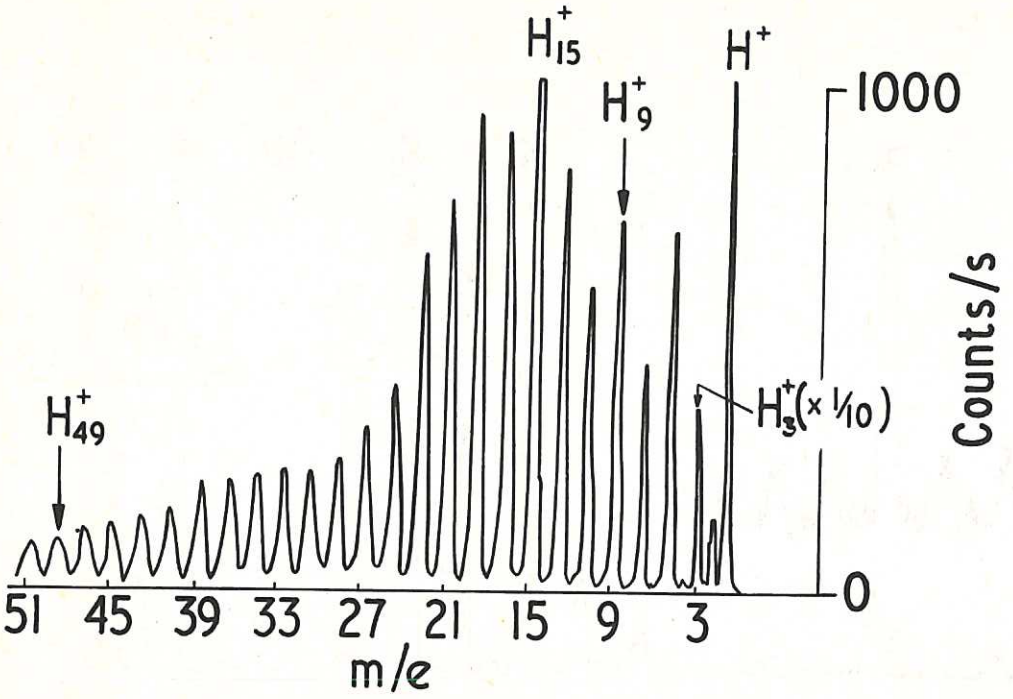

Fig.3 Ions ejected from solid H_2 by electrons

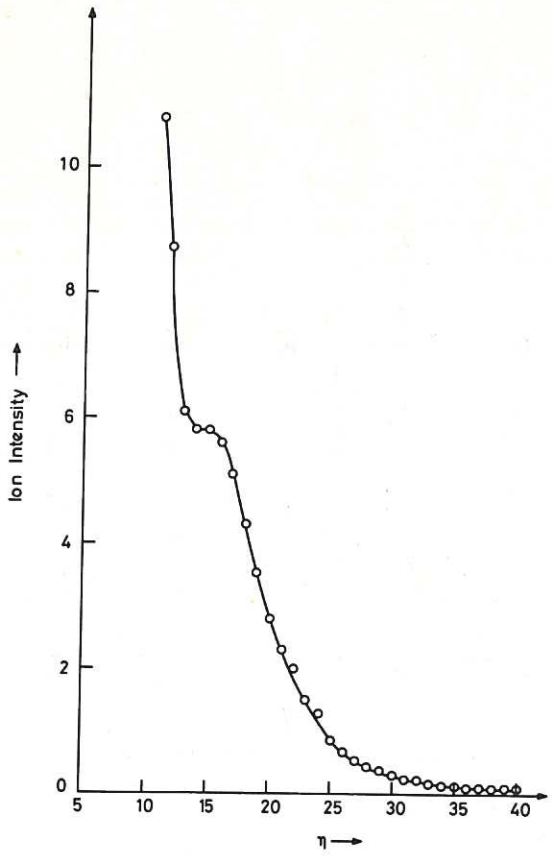

Fig.4 H_n^+ intensity distribution for $n > 10$

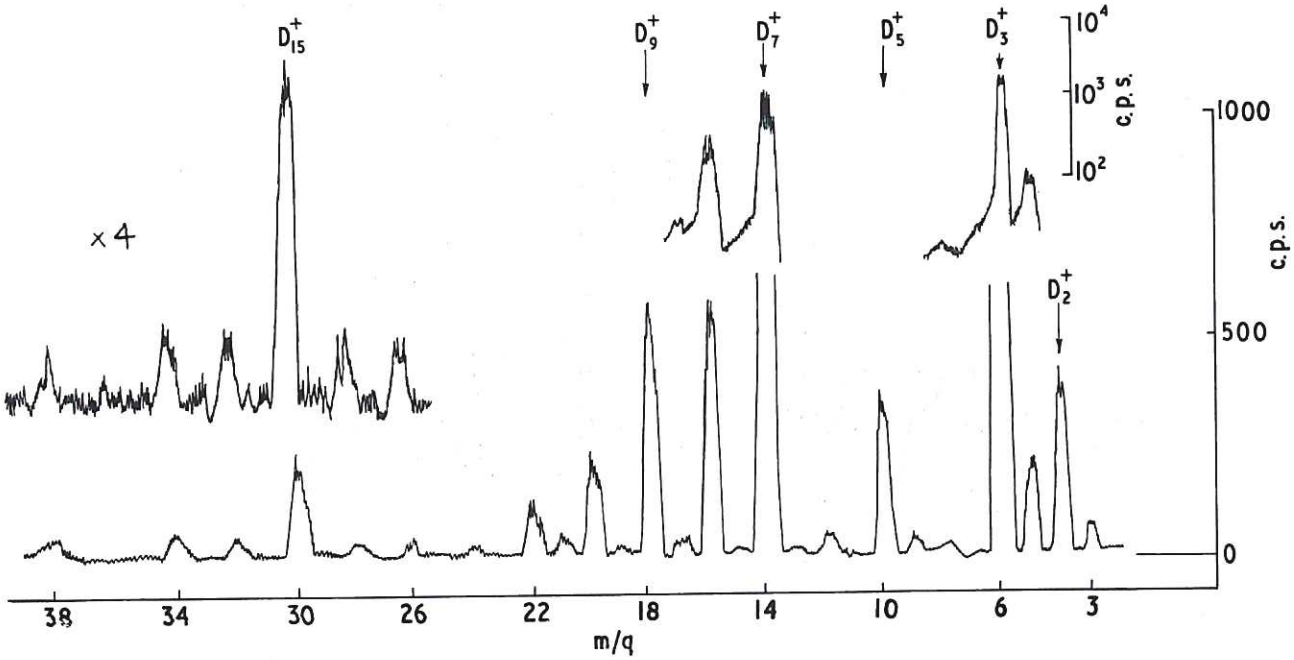

Fig.5A Deuterium ions ejected from solid D_2 by electrons

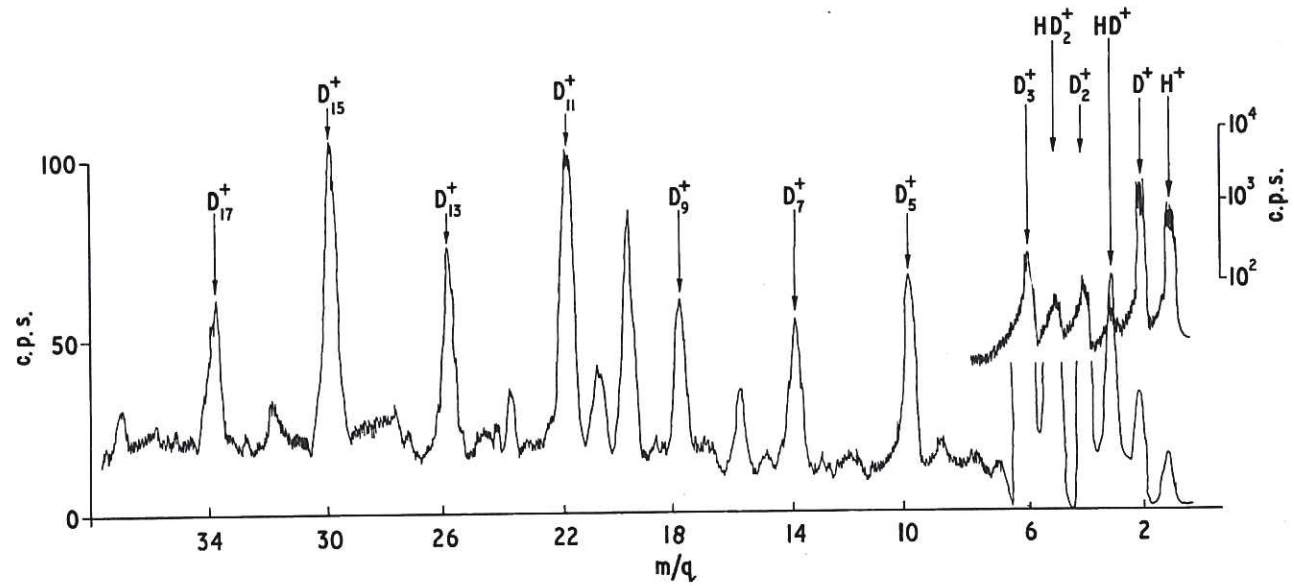

Fig.5B Deuterium ions ejected from solid D_2 by electrons

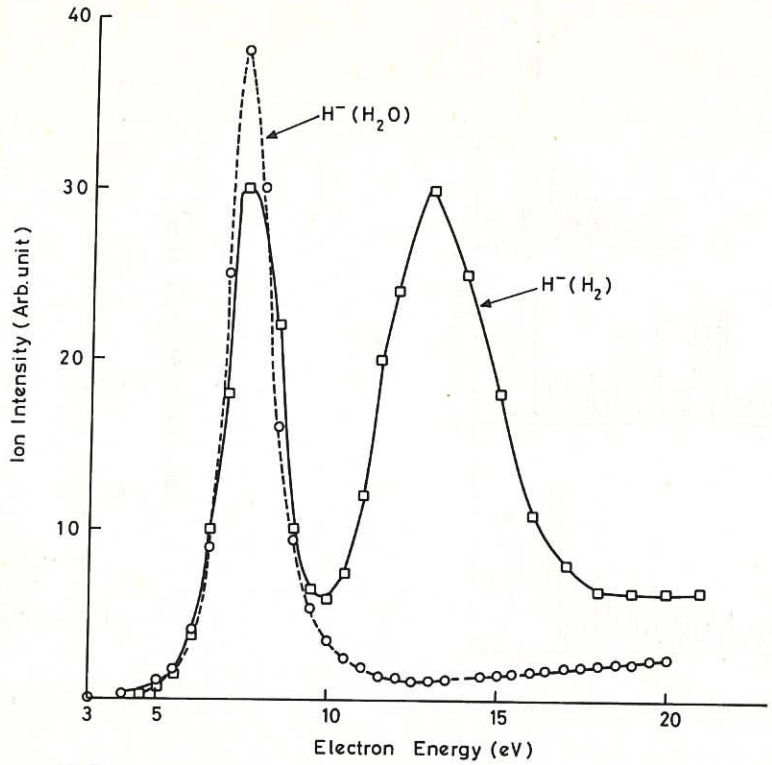

Fig.6 Variation of H^- cross-section with energy: ..... ice; ——— solid H_2

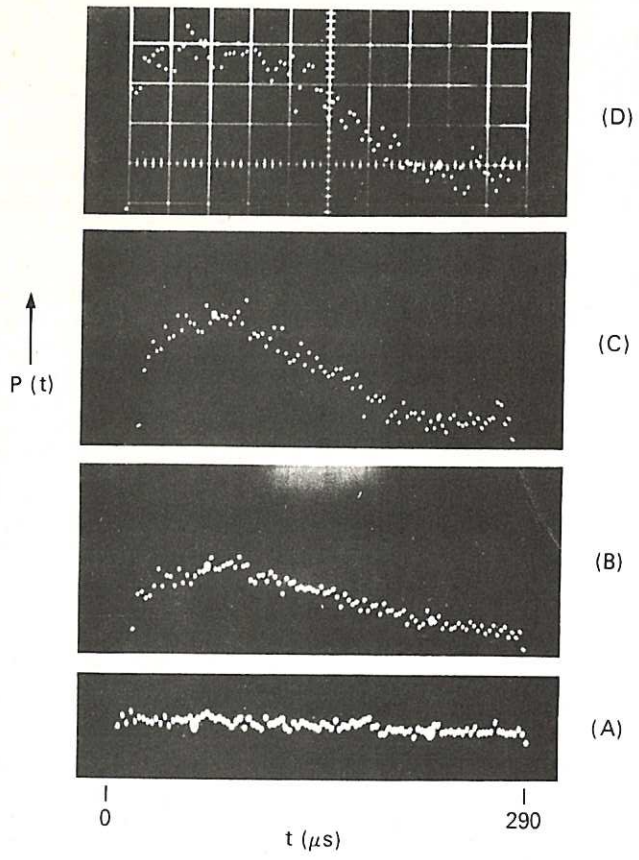

Fig.7 Time of flight distribution of H_2 from solid hydrogen: (a) background: (b) 40 eV: (c) 65 eV: (d) 90 eV electrons

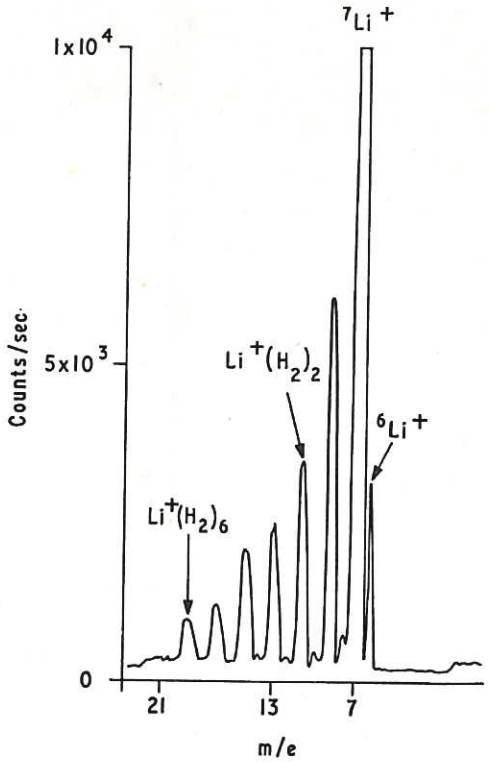

Fig.8 Clustering of H_2 on Li^+

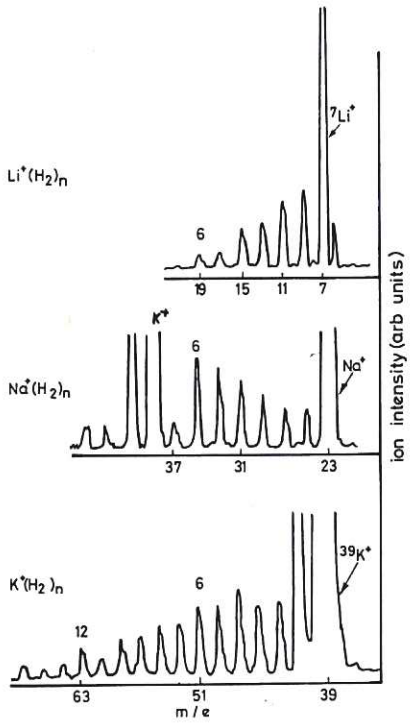

Fig.9 Alkali — hydrogen cluster ion spectra

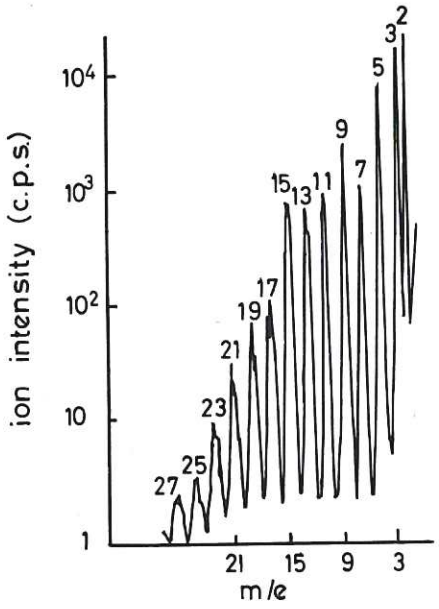

Fig.10 Mass spectra of field evaporated ions

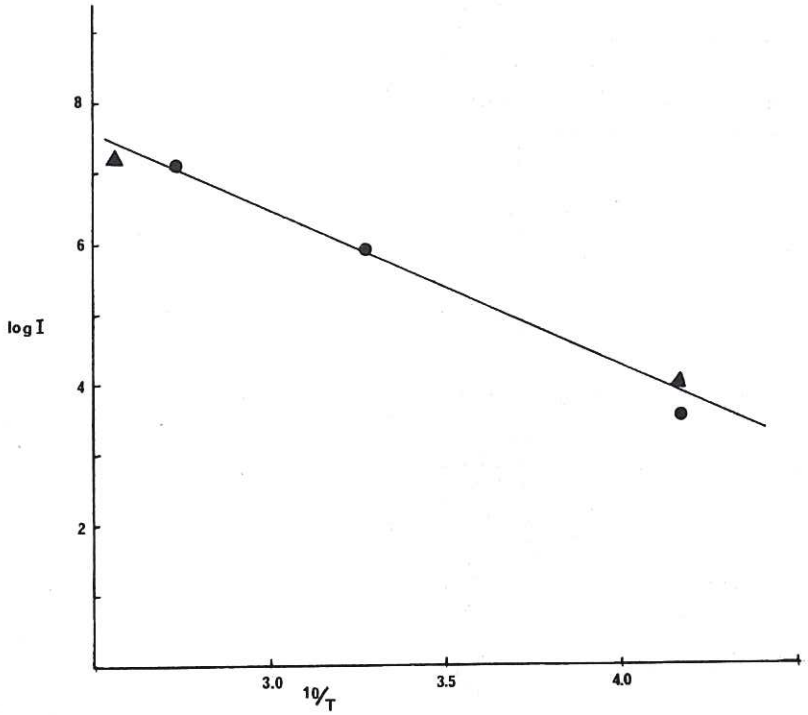

Fig.11 Temperature dependence of field evaporated ions: ▲m/e 13; ●m/e 9